

# Self-Association of Poly(*N*-isopropylacrylamide) and Its Complexation with Gelatin in Aqueous Solution

Mei Li<sup>†</sup> and Chi Wu<sup>\*,†,‡</sup>

Department of Chemistry, The Chinese University of Hong Kong, Shatin, N. T., Hong Kong, and The Open Laboratory for Bond Selective Chemistry, Department of Chemical Physics, University of Science & Technology of China, Hefei, Anhui, China

Received January 20, 1999; Revised Manuscript Received April 28, 1999

**ABSTRACT:** The association of poly(*N*-isopropylacrylamide) (PNIPAM) above its low critical solution temperature (LCST,  $\sim 32$  °C) leads to stable aggregates instead of the expected precipitation, which could be attributed to the microphase inversion of the PNIPAM chains. A laser light scattering study showed that the lower association temperature and higher PNIPAM concentration resulted in larger low density interchain aggregates with a cluster structure, while the higher association temperature and lower PNIPAM concentration led to spherical aggregates formed mainly through the packing of individual collapsed chains. Above  $\sim 32$  °C, the intrachain coil-to-globule transition competes with the interchain association. Gelatin was encapsulated/complexed into the PNIPAM aggregates and the complexation was completely reversible as the temperature varied. The PNIPAM/gelatin complexes with the highest molar mass and density were formed when the PNIPAM/gelatin weight ratio was in the range 1–2 and the temperature was close to  $\sim 32$  °C. This would be the optimum condition for the concentration of a dilute protein solution followed by the ultracentrifugation of the PNIPAM-protein complexes.

## Introduction

Protein a natural polyelectrolyte interacts strongly with both synthetic and other natural polyelectrolytes of opposite charge. Extensive studies have been devoted to the formation and structures of the protein/polyelectrolytes complexes in order to have a better understanding of the interaction of proteins inside living cells.<sup>1–10</sup> Depending on the charge density, charge distribution, chain length, chain conformation, ionic strength, and pH, the interaction between proteins and polymers may result in soluble complexes, complex coacervation,<sup>11–13</sup> or amorphous precipitates.<sup>14–16</sup> Such interactions could be used to separate different proteins and to concentrate a dilute protein solution.<sup>17–20</sup>

On the other hand, poly(*N*-isopropylacrylamide) (PNIPAM) a special kind of thermally sensitive water-soluble neutral polymer has a convenient lower critical solution temperature (LCST) at  $\sim 32$  °C; it exists as individual chains with a coil conformation at temperatures lower than  $\sim 32$  °C, but undergoes a sharp coil-to-globule transition at higher temperatures to form inter- and intrachain associations.<sup>21,22</sup> It is this convenient LCST together with its unique solution and gel properties that have recently attracted much attention.<sup>23–27</sup> It would be interesting to use these convenient LCST properties to complex PNIPAM with proteins at the temperatures slightly higher than  $\sim 32$  °C. However, to our knowledge, this has not yet been carefully studied.

In this paper, we present a systematical study of the complexation between gelatin and PNIPAM in dilute solution by a combination of static and dynamic laser light scattering, wherein the complexation was induced by the phase transition of PNIPAM at temperatures slightly higher than  $\sim 32$  °C. One of the envisioned

applications of this study is to concentrate a dilute protein or DNA solution by using ultracentrifugation because the complexation will lead to large protein/PNIPAM aggregates.<sup>28</sup> The use of PNIPAM is advantageous because of its relatively low complexation temperature and because the complexation is completely reversible when the temperature is decreased to room temperature or below.

## Experimental Section

**Sample Preparation.** Poly(*N*-isopropylacrylamide) (PNIPAM) was prepared by radical polymerization in tetrahydrofuran.<sup>29</sup> Two PNIPAM samples ( $M_w = 4.0 \times 10^4$  and  $8.44 \times 10^5$  g/mol) were used. The gelatin sample (courtesy of BASF) had a weight average molar mass of  $1.36 \times 10^5$  g/mol. The PNIPAM and gelatin samples were dissolved in deionized water. To have a complete dissolution of gelatin, 2% of formamide was added into water to break interchain hydrogen bonding. The concentrations of the PNIPAM and gelatin solutions were in the range  $2.5 \times 10^{-5}$  to  $5 \times 10^{-4}$  g/mL. All the solutions used for laser light scattering were clarified by a 0.5  $\mu$ m Millipore filter to remove dust.

**Laser Light Scattering (LLS).** We used a modified commercial laser light scattering (LLS) spectrometer (ALV/SP-150) equipped with a solid-state laser (ADLAS DPY425II, output power  $\approx 400$  mW at  $\lambda = 532$  nm) as the light source and an ALV-5000 multi- $\tau$  digital correlator. The details of the LLS instrumentation and theory can be found elsewhere.<sup>30,31</sup> In static LLS, the angular and concentration dependence of the time-average scattering intensity led to the weight average molar mass  $M_w$  and the radius of gyration ( $\langle R_g^2 \rangle_z^{1/2}$  (or written as  $\langle R_g \rangle$ ). It should be noted that in this study, the solutions were so dilute and the second virial coefficient ( $A_2$ ) was so small that the extrapolation to the zero concentration was not necessary. In dynamic LLS, the Laplace inversion or cumulant analysis of the measured intensity–intensity time correlation function resulted in the translational diffusion coefficient distribution  $G(D)$ , or further to the hydrodynamic size distribution  $f(R_h)$  by using the Stokes–Einstein equation,  $D = k_B T / (6\pi\eta R_h)$  with  $k_B$ ,  $\eta$ , and  $T$  the Boltzmann constant, the solution viscosity and the absolute temperature, respectively.

\* To whom all the correspondence should be addressed.

<sup>†</sup> The Chinese University of Hong Kong.

<sup>‡</sup> University of Science & Technology of China.

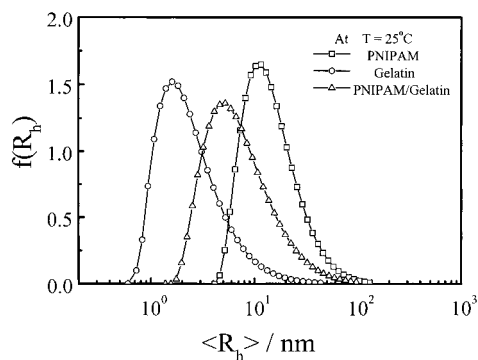


**Figure 1.** Hydrodynamic radius distributions of PNIPAM, gelatin, and the mixture of PNIPAM and gelatin at 25 °C, where the concentrations of both PNIPAM and gelatin were  $1 \times 10^{-4}$  g/mL and the concentrations of the PNIPAM and gelatin in the mixture were  $2 \times 10^{-4}$  and  $1 \times 10^{-4}$  g/mL, respectively.

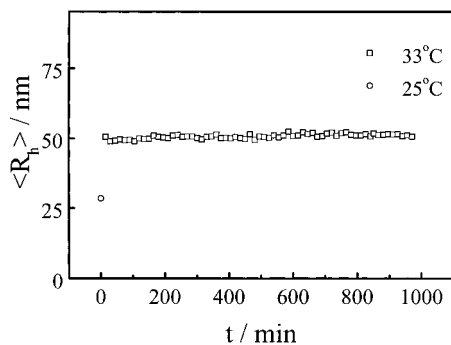
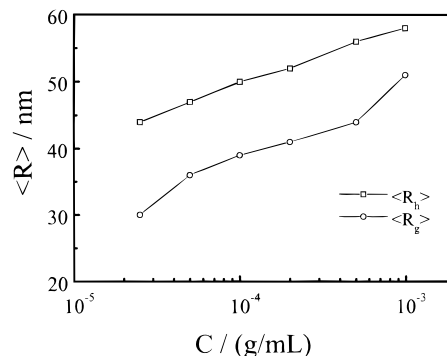


**Figure 2.** Time dependence of the average hydrodynamic radius  $\langle R_h \rangle$  of the PNIPAM aggregates after the temperature was suddenly increased from 25 to 33 °C, where the PNIPAM concentration was  $2 \times 10^{-4}$  g/mL.

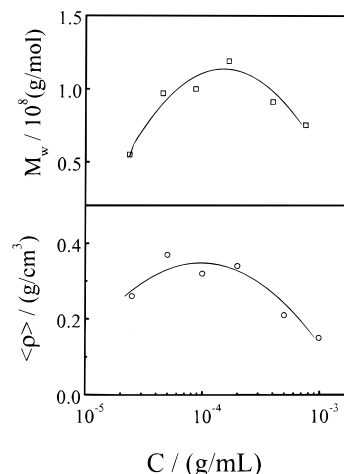
## Results and Discussion

Figure 1 shows that at 25 °C, both PNIPAM and gelatin exist as individual chains in water. The average hydrodynamic radii of gelatin and PNIPAM are  $\sim 10$  and  $\sim 30$  nm, respectively. The peak of the PNIPAM/gelatin mixture is broad and located between the peaks of individual PNIPAM and gelatin chains, indicating that no complexation occurred at this temperature. In principle, we should observe a bimodal distribution instead of a broad peak. However, dynamic laser light scattering does not resolve a mixture of two overlapping peaks. Size exclusion chromatography (SEC) confirmed that there was no PNIPAM/gelatin complexation at 25 °C.

Figure 2 shows that when the temperature was "jumped" from 25 to 33 °C, the PNIPAM chains started to aggregate so that  $\langle R_h \rangle$  increases. The increases of  $\langle R_h \rangle$  essentially stopped after half a hour, in contrast to our expected continuous growth of the aggregates with eventual precipitation. Clearly, those PNIPAM aggregates are in a metastable state. The question is how they reached this metastable state without precipitation. PNIPAM is a polymer with a delicate balance between its hydrophobic chain backbone and its hydrophilic carboxy/amide(-CONH-) group. In the phase transition, the intrachain collapse and the interchain association compete with each other. After the chains collapse into globules, the chain mobility or relaxation becomes very slow because the local chain concentration inside the globule is as high as 0.4–0.6 g/mL. Further interchain association becomes difficult because the time required for the chains inside two globules to diffuse



**Figure 3.** Concentration dependence of the average hydrodynamic radius  $\langle R_h \rangle$  and the averaged radius of gyration  $\langle R_g \rangle$  of the PNIPAM aggregates in the metastable state at 33 °C.



**Figure 4.** Concentration dependence of the weight averaged molar mass  $M_w$  and the average chain density  $\langle \rho \rangle$  of the PNIPAM aggregates in the metastable state at 33 °C.

into each other is much longer than the collision time of two globules. More important, during the collapse, more hydrophilic groups stay at the water/polymer interface, i.e., the surface of the aggregate should be slightly hydrophilic, which also prevents further inter-aggregate association. Also, the densities of water and PNIPAM are so similar that there is nearly no driving force for sedimentation under normal gravity.

As shown in Figure 3, both  $\langle R_h \rangle$  and  $\langle R_g \rangle$  increase as the PNIPAM concentration ( $C_{\text{PNIPAM}}$ ) increases. However,  $\langle R_h \rangle$  is larger, but  $\langle R_g \rangle$  is smaller, than the corresponding values ( $\langle R_h \rangle \sim 29$  nm and  $\langle R_g \rangle \sim 45$  nm) of individual PNIPAM chains at 25 °C. This reflects a combination of the intrachain coil-to-globule transition and the interchain association. The intrachain collapse reduces the size of individual chains, while the interchain association leads to large aggregates. From the definitions of  $\langle R_h \rangle$  and  $\langle R_g \rangle$ , we know that in comparison with  $\langle R_h \rangle$ ,  $\langle R_g \rangle$  is directly related to the physical space occupied by the extended polymer chain, so that the chain collapse can greatly reduce  $\langle R_g \rangle$ , while  $\langle R_h \rangle$  is less affected by the chain collapse but more influenced by interchain association. In dilute solution, the intrachain collapse was so dominant that the interchain aggregation involved mainly the packing of individual collapsed chains, resulting in a smaller  $\langle R_g \rangle$ . As the PNIPAM concentration increases, the interchain association gradually occurs prior to the intrachain collapse.

This can be better viewed in Figure 4 in terms of the concentration dependence of the weight average molar

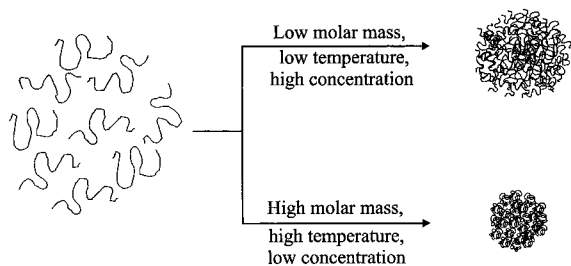


**Figure 5.** Schematic of the intrachain collapse and the interchain association of the PNIPAM chains in solution when the temperature is increased higher than its low critical solution temperature (LCST) of  $\sim 32^\circ\text{C}$ .

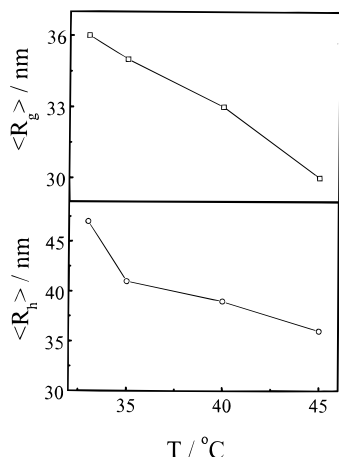


**Figure 6.** Temperature dependence of the average hydrodynamic radius ( $\langle R_h \rangle$ ) and the averaged radius of gyration ( $\langle R_g \rangle$ ) of the PNIPAM aggregates, where the PNIPAM concentration was  $5 \times 10^{-5}$  g/mL.

mass  $M_w$  and the averaged chain density  $\langle \rho \rangle$  of the aggregates. In comparison with that of individual chains, the higher values of  $M_w$  clearly demonstrate the interchain association. The average number of the PNIPAM chains inside each aggregate was in the range 40–140. The decreases of both  $M_w$  and  $\langle \rho \rangle$  at higher concentrations shows that the aggregation of the PNIPAM chains gradually switched from a dominant intrachain collapse to a dominant interchain association, as schematically shown in Figure 5.

Further, note that the ratio of  $\langle R_g \rangle / \langle R_h \rangle$  increases slightly from 0.68 to 0.88. It is known that for a uniform nondraining sphere,  $\langle R_g \rangle / \langle R_h \rangle \approx 0.774$ ; and for coiled polymer chains,  $\langle R_g \rangle / \langle R_h \rangle \sim 1.5$ . In a very dilute solution, the collapse of individual chains led to a “molten” globule structure, resembling a core–shell structure with a uniform core, but a loose shell, so that  $\langle R_g \rangle / \langle R_h \rangle < 0.774$ .<sup>32,33</sup> The slight increase of  $\langle R_g \rangle / \langle R_h \rangle$  further indicates that for the PNIPAM concentration, the intrachain-collapse dominated initial stage led to a denser core, while for the high concentration, the mixture of the interchain association and the intrachain collapse resulted in a cluster structure of low density.

Figure 6 shows that both  $\langle R_g \rangle$  and  $\langle R_h \rangle$  of the PNIPAM aggregates decrease as the temperature increases when the temperature “jumps” from  $25^\circ\text{C}$  to a higher temperature because the PNIPAM chains shrink at higher temperatures. On the other hand, Figure 7 shows that  $M_w$  decreases, but  $\langle \rho \rangle$  increases, as the temperature increases. As stated before, in the aggregation process, the interchain association makes the aggregates larger, while the intrachain coil-to-globule transition results in

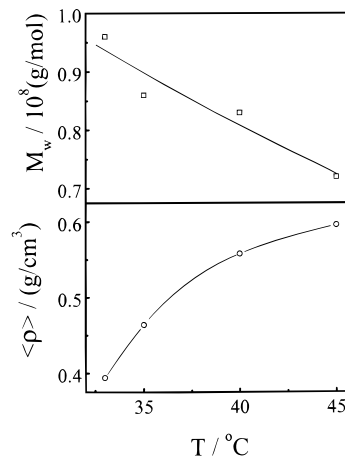


**Figure 7.** Temperature dependence of the averaged molar mass ( $M_w$ ) and the average chain density ( $\langle \rho \rangle$ ) of the PNIPAM aggregates, where the PNIPAM concentration was  $5 \times 10^{-5}$  g/mL.

**Table 1.** Concentration and Temperature Dependence of the PNIPAM Aggregation<sup>a</sup>

$T$ ( $^\circ\text{C}$ )	$C_{\text{PNIPAM}}$ (g/mL)	$\langle R_h \rangle$ (nm)	$\langle R_g \rangle$ (nm)	$\langle R_g \rangle / \langle R_h \rangle$	$M_w$ (g/mol)	$N_{\text{agg}}$	$\langle \rho \rangle$ (g/cm <sup>3</sup> )
25	$1.0 \times 10^{-4}$	31	46	1.48	$7.7 \times 10^5$	1	0.01
	$2.0 \times 10^{-4}$	29	44	1.52	$7.2 \times 10^5$	1	0.01
	$5.0 \times 10^{-4}$	28	43	1.54	$7.6 \times 10^5$	1	0.01
33	$2.5 \times 10^{-5}$	44	30	0.68	$5.5 \times 10^7$	65	0.26
	$5.0 \times 10^{-5}$	47	36	0.76	$9.7 \times 10^7$	114	0.37
	$1.0 \times 10^{-4}$	50	39	0.78	$1.0 \times 10^8$	123	0.32
	$2.0 \times 10^{-4}$	52	41	0.79	$1.2 \times 10^8$	141	0.34
	$5.0 \times 10^{-4}$	56	44	0.79	$9.1 \times 10^7$	107	0.21
35	$9.9 \times 10^{-4}$	58	51	0.88	$7.5 \times 10^7$	89	0.15
	$2.5 \times 10^{-5}$	35	28	0.80	$4.8 \times 10^7$	57	0.44
	$5.0 \times 10^{-5}$	41	35	0.85	$8.6 \times 10^7$	102	0.49
	$1.0 \times 10^{-4}$	44	38	0.86	$1.1 \times 10^8$	126	0.51
	$2.0 \times 10^{-4}$	43	35	0.81	$1.1 \times 10^8$	129	0.55
40	$5.0 \times 10^{-4}$	43	36	0.84	$8.3 \times 10^7$	98	0.41
	$9.9 \times 10^{-4}$	47	41	0.87	$6.5 \times 10^7$	77	0.25
	$2.5 \times 10^{-5}$	31	25	0.81	$3.9 \times 10^7$	46	0.52
	$5.0 \times 10^{-5}$	39	33	0.85	$8.3 \times 10^7$	99	0.55
	$1.0 \times 10^{-4}$	41	35	0.85	$9.2 \times 10^7$	109	0.53
45	$2.0 \times 10^{-4}$	40	37	0.92	$1.0 \times 10^8$	123	0.62
	$5.0 \times 10^{-4}$	41	35	0.85	$7.3 \times 10^7$	87	0.42
	$9.9 \times 10^{-4}$	43	37	0.86	$6.0 \times 10^7$	71	0.30
	$2.5 \times 10^{-5}$	31	23	0.74	$3.5 \times 10^7$	42	0.46
	$5.0 \times 10^{-5}$	36	30	0.83	$7.2 \times 10^7$	85	0.61
45	$1.0 \times 10^{-4}$	41	33	0.80	$8.7 \times 10^7$	104	0.50
	$2.0 \times 10^{-4}$	40	33	0.82	$9.4 \times 10^7$	111	0.58
	$5.0 \times 10^{-4}$	40	34	0.85	$6.5 \times 10^7$	77	0.40
	$9.9 \times 10^{-4}$	43	38	0.88	$5.2 \times 10^7$	61	0.26

<sup>a</sup> Relative errors:  $\langle R_h \rangle$ ,  $\pm 2\%$ ;  $\langle R_g \rangle$ ,  $\pm 5\%$ ;  $M_w$ ,  $\pm 5\%$ ;  $\langle \rho \rangle$ ,  $\pm 10\%$ .

smaller aggregates. After a jump to a higher temperature, the interchain association is relatively less likely than intrachain collapse. After individual chains collapse into small globules, further interchain association stops or at least becomes extremely slow, resulting in smaller aggregates with a higher density. All the results related to the concentration and temperature dependence of the PNIPAM aggregates are listed in Table 1.

Figure 8 shows that for a given PNIPAM concentration, the complexation of gelatin and PNIPAM at  $40^\circ\text{C}$  increases as the gelatin concentration increases. At the same time,  $\langle R_g \rangle / \langle R_h \rangle$  increases only slightly from 0.74 to 0.86, but  $\langle \rho \rangle$  decreases sharply from 0.32 to 0.07 g/cm<sup>3</sup>, indicating that when more hydrophilic gelatin chains were complexed with PNIPAM, the structure of the resultant complexes changed gradually from a compact globule to a loose cluster. The complexation between

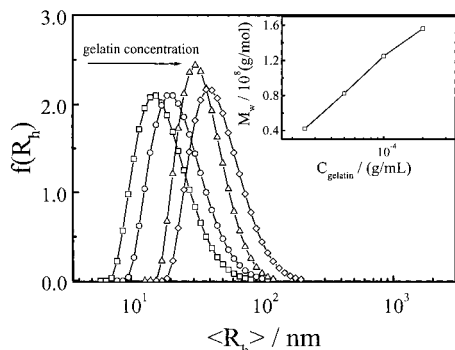


**Figure 8.** Gelatin concentration dependence of the hydrodynamic radius distribution  $f(R_h)$  and the weight averaged molar mass  $M_w$  of the PNIPAM/gelatin complexes formed at 40 °C, where the PNIPAM concentration was kept at  $1 \times 10^{-4}$  g/mL.

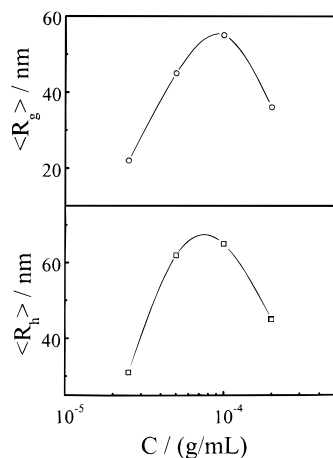
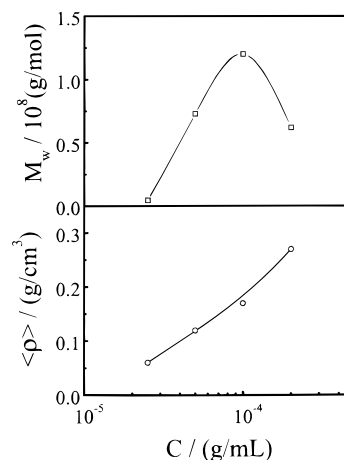


**Figure 9.** PNIPAM concentration dependence of the average hydrodynamic radius  $\langle R_h \rangle$  and the average radius of gyration  $\langle R_g \rangle$  of the PNIPAM/gelatin complexes formed at 40 °C, where the gelatin concentration was kept at  $1 \times 10^{-4}$  g/mL.

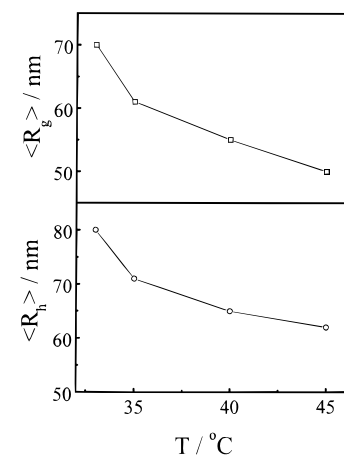
gelatin and PNIPAM can be attributed to interchain hydrogen bonding above  $\sim 32$  °C. The complexation was completely reversible when the temperature was brought back to 25 °C or below.

Figure 9 shows that if the gelatin concentration was kept at  $1 \times 10^{-4}$  g/mL, the increase of the PNIPAM concentration resulted in a more complicated picture; i.e., both  $\langle R_g \rangle$  and  $\langle R_h \rangle$  of the gelatin/PNIPAM complexes gradually increased until the PNIPAM concentration reached  $\sim 10^{-4}$  g/mL; a further increase of the PNIPAM concentration led to smaller PNIPAM/gelatin complexes, which is attributed to the competition between the association and collapse of the PNIPAM chains, because on one hand, a higher PNIPAM concentration led to larger aggregates on the basis of Figure 2; and on the other hand, more PNIPAM chains inside the complex resulted in a large shrinking force and a more compact structure. Figure 10 shows a better view of the complexation in terms of the change of  $M_w$  and  $\langle \rho \rangle$  of the gelatin/PNIPAM complexes.  $M_w$  shows the same trend as the size of the complexes, but  $\langle \rho \rangle$  increases as the PNIPAM concentration increases, indicating a more collapsed structure due to the presence of more PNIPAM chains. The ratio of  $\langle R_g \rangle / \langle R_h \rangle = 0.77\text{--}0.84$  indicates that the complexes are nearly spherical.

Figure 11 shows that for a fixed PNIPAM and gelatin concentration, an increase of temperature led to smaller PNIPAM/gelatin complexes. This shows that in order to form larger gelatin/PNIPAM complexes, the optimum



**Figure 10.** PNIPAM concentration dependence of the weight averaged molar mass  $M_w$  and the average chain density  $\langle \rho \rangle$  of the PNIPAM/gelatin complexes formed at 40 °C, where the gelatin concentration was kept at  $1 \times 10^{-4}$  g/mL.



**Figure 11.** Temperature dependence of the average hydrodynamic radius  $\langle R_h \rangle$  and the average radius of gyration  $\langle R_g \rangle$  of the PNIPAM/gelatin complexes, where the concentration of both PNIPAM and gelatin were fixed at  $1 \times 10^{-4}$  g/mL.

temperature should be as close to the LCST ( $\sim 32$  °C) as possible. In this way, the intrachain collapse slows down and the PNIPAM chains have more time to undergo interchain association before they are “frozen” by the chain collapse. By contrast, after a jump to a higher temperature, most of the PNIPAM chains undergo intrachain collapse prior to the interchain association so that smaller complexes are formed, which is also reflected in the temperature dependence of  $M_w$  as shown in Figure 12. Note that in Figure 12,  $\langle \rho \rangle$  is nearly independent of the temperature, revealing that  $\langle \rho \rangle$  is mainly influenced by the concentration of gelatin and PNIPAM.

Considering both the collapse and association of the PNIPAM chains, we expect the short chains to be very mobile and the self-wrapping of short chains into a compact globule would be more difficult. Therefore, using the low molar mass PNIPAM sample would result in larger aggregates and complexes. The results summarized in Table 2 clearly support our speculation. To concentrate a protein solution by ultracentrifugation, we need to find an optimum experimental condition at which the molar mass and density of the resultant PNIPAM/protein complexes should be as high as possible. Figure 13 shows that for the PNIPAM/gelatin ratio in the range 1–2 and the temperature close to the

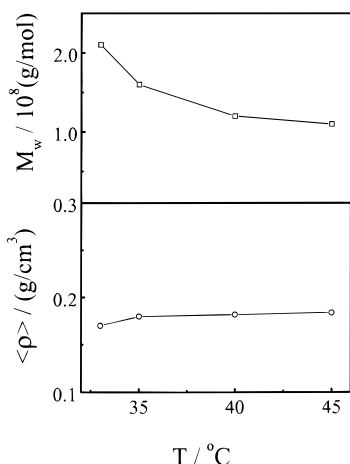


**Figure 12.** Temperature dependence of the weight averaged molar mass  $M_w$  and the average chain density  $\langle \rho \rangle$  of the PNIPAM/gelatin complexes, where the concentrations of both PNIPAM and gelatin were fixed at  $1 \times 10^{-4}$  g/mL.

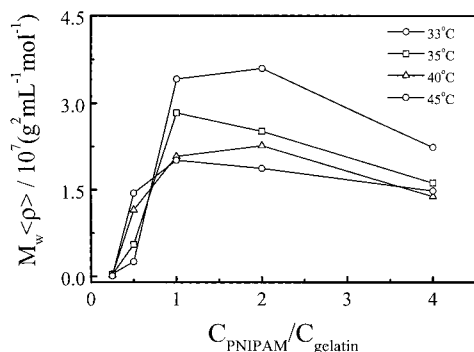


**Figure 13.** Temperature dependence of  $M_w \langle \rho \rangle$  of the PNIPAM/gelatin complexes formed with different PNIPAM/gelatin compositions.

**Table 2. Concentration Dependence of the PNIPAM Aggregates and the PNIPAM/Gelatin Complexes at 33 °C, Where PNIPAM Has a Lower Weight Average Molar Mass of  $M_w = 4 \times 10^4$  g/mol,  $T = 33$  °C**

$C_{\text{PNIPAM}}$ (g/mL)	$C_{\text{gelatin}}$ (g/mL)	$\langle R_h \rangle$ (nm)	$\langle R_g \rangle$ (nm)	$\langle R_g \rangle / \langle R_h \rangle$	$M_w$ (g/mol)	$\langle \rho \rangle$ (g/cm <sup>3</sup> )
$2.5 \times 10^{-5}$	—	87	83	0.95	$1.9 \times 10^8$	0.11
$5.0 \times 10^{-4}$	—	106	104	0.98	$4.2 \times 10^8$	0.14
$1.0 \times 10^{-4}$	—	120	109	0.91	$3.5 \times 10^8$	0.08
$2.0 \times 10^{-4}$	—	125	130	1.04	$3.6 \times 10^8$	0.07
$5.0 \times 10^{-5}$	—	139	160	1.15	$1.4 \times 10^8$	0.02
$1.0 \times 10^{-4}$	$2.8 \times 10^{-5}$	108	101	0.94	$3.1 \times 10^8$	0.10
$1.0 \times 10^{-4}$	$5.4 \times 10^{-5}$	140	132	0.94	$3.2 \times 10^8$	0.05
$1.0 \times 10^{-4}$	$1.0 \times 10^{-4}$	156	148	0.95	$4.1 \times 10^8$	0.04
$1.0 \times 10^{-4}$	$2.0 \times 10^{-4}$	197	214	1.09	$2.1 \times 10^8$	0.01
$2.5 \times 10^{-5}$	$1.0 \times 10^{-4}$	89	85	0.96	$4.2 \times 10^7$	0.02
$5.3 \times 10^{-5}$	$1.0 \times 10^{-4}$	124	117	0.94	$2.4 \times 10^8$	0.05
$1.0 \times 10^{-4}$	$1.0 \times 10^{-4}$	156	148	0.95	$4.1 \times 10^8$	0.04
$2.0 \times 10^{-4}$	$1.0 \times 10^{-4}$	161	154	0.96	$3.0 \times 10^8$	0.03

LCST,  $M_w \langle \rho \rangle$  has the highest value, favorable for separation by ultracentrifugation. The lower temperature is also favorable for preserving proteins and DNAs in their native states.

The details of the static and dynamic LLS results are summarized in Table 3. The ratios of  $\langle R_g \rangle / \langle R_h \rangle$  of the gelatin/PNIPAM aggregates are very close to  $\sim 0.8$ , except for a few cases, indicating that the complexes are uniform, nondraining and spherical. The chain density of all the aggregates is in the range  $0.04$ – $0.36$  g/cm<sup>3</sup>, much lower than the density of bulk polymers ( $\sim 1$  g/cm<sup>3</sup>), which is reasonable because a large amount of

**Table 3. Concentration and Temperature Dependence of PMIPAM/Gelatin Complexes**

$T$ (°C)	$C_{\text{PNIPAM}}$ (g/mL)	$C_{\text{gelatin}}$ (g/mL)	$\langle R_h \rangle$ (nm)	$\langle R_g \rangle$ (nm)	$\langle R_g \rangle / \langle R_h \rangle$	$M_w$ (g/mol)	$\langle \rho \rangle$ (g/cm <sup>3</sup> )
33	$1.0 \times 10^{-4}$	$2.5 \times 10^{-5}$	48	37	0.77	$7.9 \times 10^7$	0.28
	$1.0 \times 10^{-4}$	$5.0 \times 10^{-5}$	60	51	0.85	$1.4 \times 10^8$	0.26
	$1.0 \times 10^{-4}$	$1.0 \times 10^{-4}$	80	70	0.88	$2.1 \times 10^8$	0.16
	$1.0 \times 10^{-4}$	$2.0 \times 10^{-4}$	145	147	1.01	$1.4 \times 10^8$	0.02
35	$2.5 \times 10^{-5}$	$1.0 \times 10^{-4}$	37	29	0.78	$7.5 \times 10^6$	0.06
	$5.0 \times 10^{-5}$	$1.0 \times 10^{-4}$	77	64	0.83	$1.4 \times 10^8$	0.12
	$1.0 \times 10^{-4}$	$1.0 \times 10^{-4}$	80	70	0.88	$2.1 \times 10^8$	0.16
	$2.0 \times 10^{-4}$	$1.0 \times 10^{-4}$	55	47	0.85	$9.8 \times 10^7$	0.23
	$1.0 \times 10^{-4}$	$2.5 \times 10^{-5}$	41	30	0.73	$5.3 \times 10^7$	0.30
	$1.0 \times 10^{-4}$	$5.0 \times 10^{-5}$	54	44	0.81	$1.0 \times 10^8$	0.25
	$1.0 \times 10^{-4}$	$1.0 \times 10^{-4}$	71	61	0.86	$1.6 \times 10^8$	0.18
	$1.0 \times 10^{-4}$	$2.0 \times 10^{-4}$	112	84	0.75	$1.4 \times 10^8$	0.04
40	$2.5 \times 10^{-5}$	$1.0 \times 10^{-4}$	34	25	0.74	$5.7 \times 10^6$	0.06
	$5.0 \times 10^{-5}$	$1.0 \times 10^{-4}$	67	62	0.92	$9.8 \times 10^7$	0.13
	$1.0 \times 10^{-4}$	$1.0 \times 10^{-4}$	71	61	0.86	$1.6 \times 10^8$	0.18
	$2.0 \times 10^{-4}$	$1.0 \times 10^{-4}$	48	39	0.81	$6.7 \times 10^7$	0.24
	$1.0 \times 10^{-4}$	$2.5 \times 10^{-5}$	37	28	0.76	$4.2 \times 10^7$	0.33
	$1.0 \times 10^{-4}$	$5.0 \times 10^{-5}$	49	40	0.82	$8.2 \times 10^7$	0.28
	$1.0 \times 10^{-4}$	$1.0 \times 10^{-4}$	65	55	0.85	$1.2 \times 10^8$	0.17
	$1.0 \times 10^{-4}$	$2.0 \times 10^{-4}$	96	82	0.85	$1.6 \times 10^8$	0.07
	$2.5 \times 10^{-5}$	$1.0 \times 10^{-4}$	31	22	0.71	$4.5 \times 10^6$	0.06
	$5.0 \times 10^{-5}$	$1.0 \times 10^{-4}$	62	45	0.72	$7.3 \times 10^7$	0.12
	$1.0 \times 10^{-4}$	$1.0 \times 10^{-4}$	65	55	0.85	$1.2 \times 10^8$	0.17
	$2.0 \times 10^{-4}$	$1.0 \times 10^{-4}$	45	36	0.80	$6.2 \times 10^7$	0.27
45	$1.0 \times 10^{-4}$	$2.5 \times 10^{-5}$	35	27	0.77	$4.0 \times 10^7$	0.36
	$1.0 \times 10^{-4}$	$5.0 \times 10^{-5}$	47	35	0.74	$7.0 \times 10^7$	0.27
	$1.0 \times 10^{-4}$	$1.0 \times 10^{-4}$	62	50	0.81	$1.1 \times 10^8$	0.18
	$1.0 \times 10^{-4}$	$2.0 \times 10^{-4}$	89	73	0.82	$1.6 \times 10^8$	0.09
	$2.5 \times 10^{-5}$	$1.0 \times 10^{-4}$	31	23	0.74	$2.8 \times 10^6$	0.04
	$5.0 \times 10^{-5}$	$1.0 \times 10^{-4}$	58	52	0.90	$7.5 \times 10^7$	0.15
	$1.0 \times 10^{-4}$	$1.0 \times 10^{-4}$	62	50	0.81	$1.1 \times 10^8$	0.18
	$2.0 \times 10^{-4}$	$1.0 \times 10^{-4}$	45	37	0.82	$6.3 \times 10^7$	0.27

water is still enclosed inside the complexes. The complexes formed at higher temperatures have a more compact structure with a higher chain density due to the collapse of the PNIPAM chains. The lower density of the gelatin/PNIPAM complexes indicates that the hydrophilic gelatin chains inside the complexes partially prevent the collapse of the PNIPAM chains, resulting in a relatively looser cluster structure.

**Acknowledgment.** The financial support of the National 973 Project (RE-05-02), the Research Grants Council of Hong Kong Special Administration Region Earmarked Grant 1998/99 (CUHK 4123, 2160111), and National Distinguished Young Investigator Grant (1996, 29625410) is gratefully acknowledged.

## References and Notes

- Morawetz H.; Hughes W. L. *J. Phys. Chem.* **1952**, *56*, 64.
- Berdick M. Morawetz H. *J. Biol. Chem.* **1954**, *206*, 959.
- Morawetz H.; Sage, *Arch. Biochem. Biophys.* **1955**, *56*, 103.
- Bowman, W. A.; Rubinstein, M.; Tan, J. S. *Macromolecules* **1997**, *30*, 3262.
- Mattison, K. W.; Dubin, P. L.; Brittain, I. J. *J. Phys. Chem. B* **1998**, *102*, 3830.
- Tribet, C.; Audebert, R.; Popot, J.-L. *Langmuir* **1997**, *13*, 5570.
- Tribet, C.; Porcar, I.; Bonnefont, P. A.; Audebert, R. *J. Phys. Chem. B* **1998**, *102*, 1327.
- Nath, S.; Patrickios, C. S.; Hatton, T. A. *Biotechnol. Prog.* **1995**, *11*, 99.
- Xia, J.; Dubin, P. L.; Dautzenberg, H. *Langmuir* **1993**, *9*, 2015.
- Xia, J.; Dubin, P. L.; Kim, Y.; Muhoberac, B. B.; Klimkowski, V. J. *J. Phys. Chem.* **1993**, *97*, 4528.
- Lenk, T.; Thies, C. In *Coulombic Interactions in Macromolecular Systems*; Eisenberg, A., Bailey, F. E., Eds.; American Chemical Society: Washington, DC, 1987; Chapter 8.

- (12) Veis, A. *Am. Chem. Soc., Div. Polym. Chem. Prepr.* **1991**, *32*, 596.
- (13) Burgess, D. J.; Carless J. E. *J. Colloid Interface Sci.* **1984**, *98*, 1.
- (14) Nguyen, T. Q. *Makromol. Chem.* **1986**, *187*, 2567.
- (15) Sternberg, M.; Hershberger, C. *Biochim. Biophys. Acta* **1974**, *342*, 195.
- (16) Kokufuta, E.; Shimizu, H.; Nakamura, I. *Macromolecules* **1981**, *14*, 1178.
- (17) Fisher, R. R.; Glatz, C. E. *Biotechnol. Bioeng.* **1988**, *32*, 777.
- (18) Bozzano, A. G.; Andrea, G.; Glatz, C. E. *J. Membr. Sci.* **1991**, *55*, 181.
- (19) Clark, K. M.; Glatz, C. E. *Biotechnol. Prog.* **1987**, *3*, 241.
- (20) Stregge, M. A.; Dubin, P. L.; West, J. S.; Daniel Flinta, C. D. In *Protein purification: From molecular mechanisms to large-scale processes*; Ladisch, M., Willson, R. C.; Painton, C. C., Builder, S. E., Eds.; ACS Symposium Series 427; American Chemical Society: Washington, DC; Chapter 5.
- (21) Wu, C.; Zhou, S. *Macromolecules* **1995**, *28*, 5388.
- (22) Wu, C.; Zhou, S. *Macromolecules* **1995**, *28*, 8381.
- (23) Wu, C.; Qiu, X. *Macromolecules* **1997**, *30*, 7921.
- (24) Kidchob, T.; Kimura, S.; Imanishi, Y. *J. Chem. Soc., Perkin Trans.* **1997**, *2*, 2195.
- (25) Hu, Z.; Chen, Y.; Wang, C.; Zheng, Y.; Li, Y. *Nature* **1998**, *393*, 149.
- (26) Hino, T.; Prausnitz, J. M. *Polymer* **1988**, *39*, 3279.
- (27) Bergbreiter, D. E.; Case, B. L.; Liu, Y.; Caraway, J. W. *Macromolecules* **1998**, *31*, 6053.
- (28) Umeno, D.; Kawasaki, M.; Maeda, M. *Bioconjugate Chem.* **1998**, *9*, 719.
- (29) Zhou, S.; Fan, S.; Au-yeung, S.; Wu, C. *Polymer* **1995**, *36*, 1341.
- (30) Chu, B. *Laser Light Scattering*, 2nd ed.; Plenum Press: New York, 1991.
- (31) Pecora, R. *Dynamic Light Scattering*; Plenum Press: New York, 1976.
- (32) Wu, C.; Zhou, S. *Phys. Rev. Lett.* **1996**, *77*, 3053.
- (33) Wang, X.; Qiu, X.; Wu, C. *Macromolecules* **1998**, *31*, 2972.

MA990085S